The ballast pick-up problem. A theoretical approach and two experimental campaigns

Fermin Navarro-Medina[a], Angel Sanz-Andres[b], Isabel Perez-Grande[c], Alejandro Martinez[d], Enrique Vega[e], Miguel Rodriguez-Plaza[f], Ignacio Jorge Iglesias-Dia[g], Alvaro Andres-Alguacil[h], Diana Alonso-Gimeno[i]

IDR/UPM, E.T.S.I. Aeronáuticos, Universidad Politécnica de Madrid. Plaza del Cardenal Cisneros, 3. E-28040, Madrid, Spain. Tel. +34 91 336 6353 Fax. +34 91 336 6353
[a]fermin.navarro@upm.es,[b]angel.sanz.andres@upm.es,[c]isabel.perez.grande@upm.es,
[d]alejandro.martinez@upm.es, [e]e.vega@upm.es

ADIF, Administrador de Infraestructuras Ferroviarias. Technological Innovation Direction. Titán, St 4, 2nd floor, 28045 Madrid, Spain, Tel. +34690802566
[f]mrodriguez@adif.es,[g]Jorge.Iglesias@adif.es,[h]Alvaro.andres@adif.es,[i]dalonso@adif.es

1 INTRODUCTION

The aim of this contribution is to present a theoretical approach and two experimental campaigns (on wind tunnel and on the track) concerning the research work about the ballast train-induced-wind erosion (BTIWE) phenomenon. When a high speed train overpasses the critical speed, it produces a wind speed close to the track large enough to start the motion of the ballast elements, eventually leading to the rolling of the stones (Kwon and Park, 2006) and, if these stones get enough energy, they can jump and then initiate a saltation-like chain reaction, as found in the saltation processes of soil eolian erosion (Bagnold, 1941). The expelled stones can reach a height which is larger than the lowest parts of the train, striking them (and the track surroundings) producing considerable damage that should be avoided. There is not much published work about this phenomenon, in spite of the great interest that exists due to its relevant applications in increasing the maximum operative train speed. Particularly, the initiation of flight of ballast due to the pass of a high speed train has been studied by Kwon and Park (2006) by performing field and wind tunnel experiments. These authors have developed also a simple mathematical model of the trajectory, once the motion has started, that is, without considering the phase of rotational motion initiation. Quinn et al. (2009) made reference to the mechanism of initiation of the ballast particle flight, which requires that the ballast particle acquires some vertical velocity component to start the flight, as it has been also pointed out in some previous experiments concerning saltation processes of soil eolian erosion, as for instance in Owen (1964), Nalpanis et al. (1993) and Zhang et al. (2007). Before the initiation of flight, a roll-jump process of the ballast stones has been found by Kwon and Park (2006). The initial rotation, together with the rolling-jumping phase, is an intermediate phase between the initial equilibrium and the final flight, phase that is more relevant in the case of a time-varying, gusty flow, like the one generated by the passing train. In relation with this intermediate phase, a new theoretical approach concerning the determination of the conditions for the initiation of the motion of the ballast stones due to the wind gust created under the high-speed trains has been recently developed (Sanz-Andres and Navarro-Medina, 2010).

Besides the theoretical model, two experimental campaigns have been performed: one in the gust wind tunnel, which has been developed at the IDR/UPM facilities, and the other one on the field, that is at the railroad track. In the gust wind tunnel test section the maximum wind speed is some 20 m/s and the maximum gust frequency is 10 Hz. The test section is 0.39 m × 0.54 m, which is suitable to perform experiments with stone models. In the

range of parameters explored, the experimental results show a good agreement with the theoretical model predictions. The other experimental campaign presented at this contribution has been developed at the railroad track at kp 69.500 Madrid – Barcelona High Speed Line, where the ADIF´s Brihuega (Guadalajara) test building is placed. The experimental approach selected to study the effect on the ballast of the flow generated by the train is the measurement of the pressure load due to this flow acting on a body, which is divided in two parts (a semicircular cylinder and a vertical wall). The body is equipped with pressure taps and placed on the ballast.

In this contribution the theoretical model is summarized, the experimental facilities at the wind tunnel and at the railroad track are described, and the experimental results are compared with the theoretical predictions.

2 THEORETICAL MODEL

In this section the mathematical model of the initiation of the stone motion developed by Sanz-Andres and Navarro-Medina (2010) is summarized. The model is based on the stone rotational dynamics equation, which is formulated taking into account both gravity and aerodynamic forces. These aerodynamic forces are the result of the interaction of the train-generated gust impinging the stones lying on the track. Although the aerodynamic forces are intrinsically non steady, under some conditions a quasi-steady aerodynamic model can be employed. As a result of the model, the condition for the start of the motion is obtained, which contains the Tachikawa number (a kind of Froude number). Besides, the role of the aerodynamic characteristics of the stone is clarified, which is described in terms of the zero aerodynamic moment line of the stone, ZML (Fig. 1), and the aerodynamic moment coefficient, c_m.

As the problem is a very complex one, in a first approach it should be simplified at some suitable extend. Therefore, it is assumed that the stone, which is lying on a horizontal wall, can rotate around the rearward supporting contact point A, due to the action of the aerodynamic loads produced by a time-dependent incoming flow $U(t)$, while restrained by the action of the gravity forces. If the stone has some previous sliding motion over the sleeper or other stones in the ballast bed, it is assumed that this sliding motion will be blocked by the physical interference at this rearward supporting contact point (RSCP), and only rotation around RSCP will be allowed from this instant onwards. The dynamics of the stone is described by the equation of the angular acceleration produced by the applied torque:

$$\ddot{\theta}_L = \frac{1}{I}\left[\frac{1}{2}\rho_a A_{Fp} R U^2(t) c_m(\theta_L) - M_p g d_{cm\mathrm{A}} \cos\theta_{cm}\right], \tag{1}$$

where I is the moment of inertia with regard to point A, ρ_a the air density, A_{Fp} the plan form area, R the characteristic stone dimension (e.g. radius of the sphere circumscribing the stone), c_m the coefficient of aerodynamic moment with regard to point A, M_p the stone mass, g the acceleration of gravity, $d_{cm\mathrm{A}}$ the distance between the centre of mass and the pivoting point A, $\theta_{cm} = \theta_L + \delta_{Lcm}$, δ_{Lcm} the angle between the ZML and the centre of mass line, $\theta_L = \beta + \delta_{CL}$, β the angle between a stone reference chord and the horizontal plane, δ_{CL} the angle between the stone chord and the ZML, $U(t) = U_0 \cdot f(t)$, and U_0 is the time-averaged incoming speed.

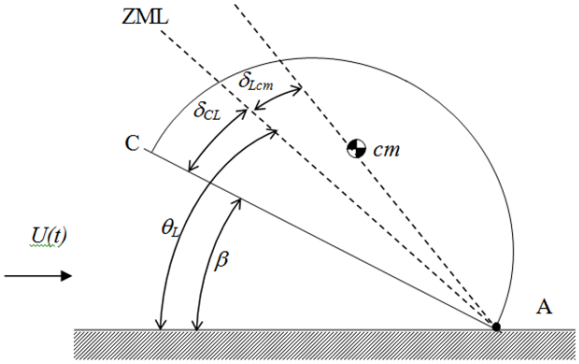

Figure 1. Sketch of the stone model configuration considered. Definition of angles. ZML: zero moment line; cm: centre of mass; and CA: chord of the body.

The first term inside the brackets of Equation 1 is the aerodynamic moment, with regard to point A, assuming a quasi-steady behavior. The second term is just the moment of the gravity forces, with regard to point A. Once the solution of the dimensionless and linear version of Equation 1 is obtained, it can be shown that if the stone is at rest at the initial time, with increasing acceleration, that is $\theta_0' = \theta_0'' = 0$ and $\theta_0''' > 0$ with θ_0 the initial stretched angular position of ZML, the stability condition is reduced to

$$|\theta_0| \geq |\theta_{0\text{lim}}| = \frac{2}{\sqrt{1+X}}, \quad X \cong \frac{\Omega^2}{K_0 c_{m\alpha}}. \tag{2}$$

This stability condition depends on the parameter X, which includes the dimensionless gust frequency, $\Omega = 2\pi / (t_{cn} / t_{crg})$, where t_{cn} is the characteristic time of the gust and $t_{crg} = \sqrt{I / (M_p g d_{cmA})}$ is the characteristic time of the stone rotational motion due to gravity; the Tachikawa number, $K_0 = \rho_a A_{Fp} U_0^2 R / (2 M_p g d_{cmA})$; and the slope of the curve of coefficient of aerodynamic moment with regard to point A vs angle of attack, $c_{m\alpha}$. It is found that two limits exist, for long and short duration gusts, respectively. The limit cases for the gust effect are:

- Limit *L*) long duration gust $X \to 0$ ($t_{cn} >> t_{crg}$), $\theta_{L\text{lim}L} = \theta_{Lm}$ (1- 2 ε), and
- Limit *S*) short duration gust $X \to \infty$ ($t_{cn} << t_{crg}$), $\theta_{L\text{lim}S} = \theta_{Lm} = 1 / (K_0\, c_{m\alpha})$

In the case of long duration gusts, the effect is the same as that of a quasi-steady flow, that is, the instantaneous speed can be taken as a permanent speed, and then the effect on aerodynamic moment is 1+2 ε, therefore, the limit value is the equilibrium at maximum speed. In the case of short duration gust, the limit angle is due to the mean value of the aerodynamic force, as the stone-flow system behaves like a strange kind of low pass filter.

3 EXPERIMENTAL SET-UP AND RESULTS

An experimental campaign has been developed at a gust wind tunnel with the objectives of validating the theoretical predictions, and of obtaining the influence on the stability condition (2) of some parameters involved in the BTIWE phenomenon while the others are controlled. On the other hand, other campaign has been developed on the high speed railroad track Madrid-Barcelona in order to study the effect on the track ballast of the flow generated by the train.

3.1 *Gust wind tunnel*

A wind tunnel equipped with a gust generation mechanism has been developed, as part of the research program on the BTIWE phenomenon generated by high speed trains. The objective is to study the initiation of motion of a ballast stone model lying on the wind tunnel chamber floor due to the aerodynamic force produced by a time-dependent wind. If this force is large enough, the body could start to rotate around the RSCP of the stone, which is fixed to the floor.

Air flow in the wind tunnel is generated by two 0.66 m diameter centrifugal fans (Tecnifan TSA-serie R), which are positioned together, one above the other, powered by two 15 kW electrical motors, controlled by a MOELLER DV6-340-15k frequency inverter. Air is propelled by these fans (Fig. 2) through a 0.8 m length transition chamber followed by a 2 m length test chamber. Both chambers are made with wooden plates, which are attached to a metallic duct structure. The structure is equipped with wheels mounted on rails fixed to the floor, so that, the whole ensemble can be moved along the axial direction in order to facilitate the operations inside the test chamber. The working chamber is divided vertically into two equal parts by means of a horizontal wooden wall. Each part is 0.54 m width and 0.39 m height. The gust generation is based on a periodic pressure drop concept applied alternatively to the two contiguous test chambers. To achieve the alternative pressure drop, a turning gate is located at the downstream extreme of each test chamber, in such a way that the phase angle difference is 90 degrees. Therefore, at the time instant when the upper gate blocks the corresponding cross section the lower gate is completely open, allowing the air to freely flow. As a consequence, the gust generation system produces a flow that goes alternatively through either the upper or lower chamber. Each turning gate is composed of two rectangular steel plates 1 mm thick and 380 mm × 520 mm sides, which are screwed to 3 steel support tubes of 360 mm length and 15 mm × 25 mm rectangular section, fixed to the rotation axis. The steel plates can be positioned at different places along the support tubes, so that the gate chord can be modified, leading to larger or smaller test section blockage ratio. The turning gate rotation axes are mounted on bearings. One gearwheel is mounted at one end of each gate axis. These two gears are engaged to each other, and to a third gearwheel mounted on the axis of a direct current electric motor, by using a roller chain. A 355 mm × 301 mm rectangular polymethyl methacrylate window is placed in the lower test chamber wall at the appropriate axial position to allow for a good visibility of the stone models during tests. The lower test chamber can be accessed through a gate placed on the floor, to facilitate the mounting of the models. All stone models are mounted in wooden base plates, placed close to the window, on the lower test chamber floor, using the access gate.

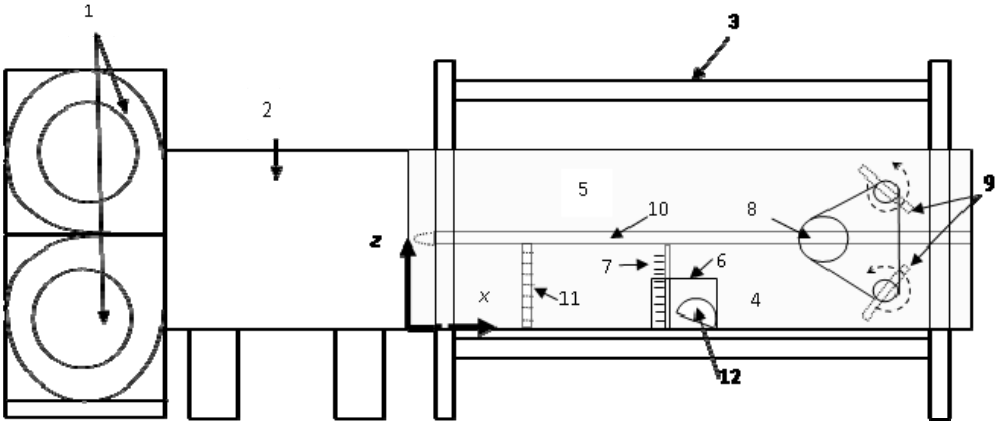

Figure 2. Sketch of the wind tunnel with the gust generation system: 1) centrifugal fans; 2) transition chamber; 3) metallic duct structure; 4) and 5) lower and upper test chamber, respectively; 6) test section window; 7) pressure probe rake; 8) gust motor; 9) turning gates and gearwheels; 10) test chamber splitter plate; 11) flow quality conditioning elements; and 12) stone model.

Tests devoted to the determination of the successful initiation of motion of a hemispherical stone model have been performed, whose results are plotted in Figure 3. In the same figure a picture of the stone model placed in the test chamber is presented. The limit angle between the horizontal plane and the Zero Momentum Line, θ_{Llim}, is plotted against the parameter $K_0 c_{m\alpha}$. Theoretical calculations based on Equation 2 are also plotted in Figure 3 together with the experimental results. In the theoretical model, two limit cases were predicted: the low frequency gust case (lower limit), and the steady speed case (upper limit), which coincides with the high frequency gust case. To check this result, three values of the frequency of turning gate rotation are displayed for both theoretical predictions and experimental results as follows: the steady case, a low frequency gust and a high frequency one. The three resultant experimental curves appear in the expected order as predicted by the theoretical model: the steady case curve as the upper limit, the low frequency case curve in the lower position, and the high frequency case curve in the middle. Besides, as velocity increases, experimental results show a better agreement with theoretical predictions, as a consequence of the better accuracy of the linearized model in the high speed, low angle of attack range.

This experimental configuration inside the wind tunnel is similar, but simplified, to the situation in the railway track of a ballast stone lying on a sleeper (or railroad tie). In the wind tunnel configuration, the values of stone characteristics, such as the mass and dimensions of the stone, and its orientation respect to wind direction, and wind characteristics, as mean speed, frequency and amplitude of a single-frequency gust and turbulence intensity are known and controllable, unlike the situation in the railway track. In the real BTIWE problem, the parameters neither do have well specified values of size, shape, mass or position, nor they are deterministic (e.g. the gust frequency), although they could be described with appropriate probability density functions. Therefore, the continuation of the work should be based mainly on statistical analysis, although taking into account also the Equation 2 for the stability limits deduced from the present deterministic studies, as advanced in Sanz-Andres and Navarro-Medina (2010).

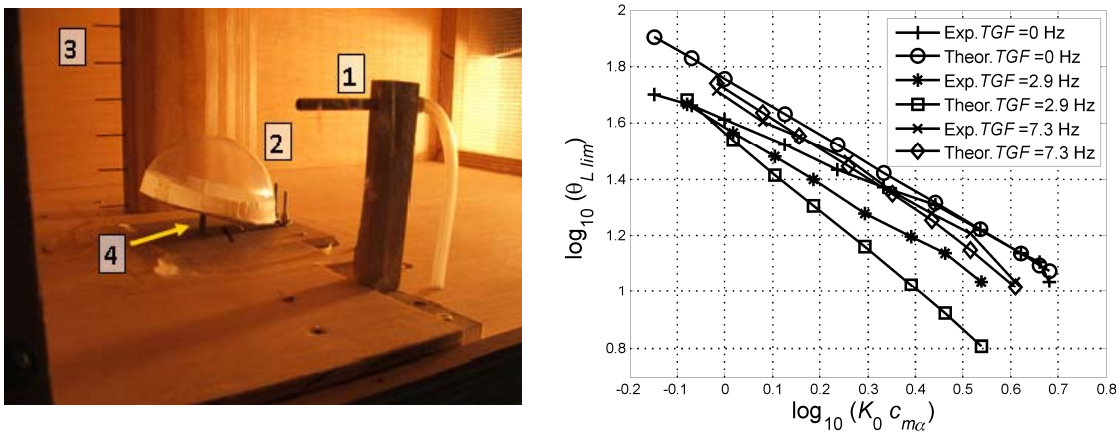

Figure 3. Left side: photograph of the testing area of the gust wind tunnel showing the reference total pressure probe (1), the semi-spherical stone model (2), the total pressure-probe rake (3) and the screwed rod, which is the supporting point for the stone model (4). The air flow is from left to right. Right side: Experimental results and theoretical predictions. Variation with the parameter $K_0 c_{m\alpha}$, of the angle between the horizontal plane and the Zero Momentum Line at the successful motion initiation instant, θ_{Llim}.

3.2 *On track experiments*

In these tests the pressure load due to the flow generated by the train, which is acting on a body equipped with pressure taps and placed on the ballast is measured. In parallel with the

pressure measurements, the wheel passes are also detected by using a light barrier, in order to synchronize the pressure measurements with the actual train geometry. The vertical acceleration on the center of the sleeper is also recorded, aiming at to obtain experimental data that can help to the study of the action of the sleeper vibration on the initiation of the rotation of the ballast lying on it.

These measurements have been carried out in the ADIF´s Brihuega (Guadalajara) test building, placed at kp 69.500 Madrid – Barcelona High Speed Line, on the tracks 1 and 2. These experiments have been developed during the period between October 26th of 2010 and March 23th of 2011.

Pressure measurements have been obtained on a stone simulating wooden body that is divided in two parts, each one shaped with two-dimensional geometry. One of them is a 6 cm diameter hemi-cylindrical stone model, and the other part is a 3 cm height and 2 cm width vertical wall. The whole body has been placed on a plane wooden surface, which is high leveled with the upper surface of the sleeper and it is considered as reference plane for the flow. Below this surface a parallelepiped box houses the pressure transducers and the accelerometer amplifiers. The box has been buried within the ballast stones at the space between two sleepers. At the hemi-cylindrical part of the stone model five taps have been arranged, including the reference tap, two taps on the upper part of the hemi-cylinder, and two taps at the reward side. These taps have been arranged in pairs in order to provide redundancy. In the middle of the two parts of the test model a kind of reversible Pitot probe was placed at 50 mm high respect to the reference plane. At the base of the vertical wall, two pressure taps are placed at windward side of the wall and two taps at the leeward side to measure the pressure jump across the vertical wall.

The value of the non-dimensional pressure coefficient c_{p0j} was used, that is obtained as the value of the pressure difference between each tap and its corresponding reference tap, divided by the dynamic head (dynamic pressure) referred to the train speed U_T and the air density ρ_a,

$$c_{p0j} = -\frac{p_j - p_r}{\frac{1}{2}\rho_a U_T^2}, \tag{3}$$

where j = 1, 2, ... This pressure coefficient is not the usual at aerodynamics field, where the reference pressure p_r is the static pressure and the dynamic pressure is referred to the incoming flow speed, but they are difficult to be measured at the space between the railroad track and the lower parts of the train.

In order to obtain some simplified results from the on track campaign, the pressure peaks are analyzed considering those that can transmit enough energy to the ballast stone in a short time in which the static conditions can be valid, as the angle of attack between the stone chord and the horizontal plane is small. Therefore the angular impulse, S_n, can be calculated as the closed area between the curve of the pressure coefficient variation with time and the pressure coefficient threshold, c_{pl}, that is the ratio of the stone weight and the dynamic head of the wind gust generated by the train. By using the data of enough number of passes of the same train model in a given track, the histograms of the angular impulse have been obtained. From these histograms, the values of the extreme angular impulses in each pass $S_{n,crit}$ (the one which appears just one time) are compared with the corresponding values for the other cases with different trains, tracks, taps, and c_{pl}. An example for one of the pressure taps is shown in Figure 4, where four trains 1, 2, 3, and 4, are compared for both tracks V1 and V2 and for two values of c_{pl} (0.2 and 0.4).

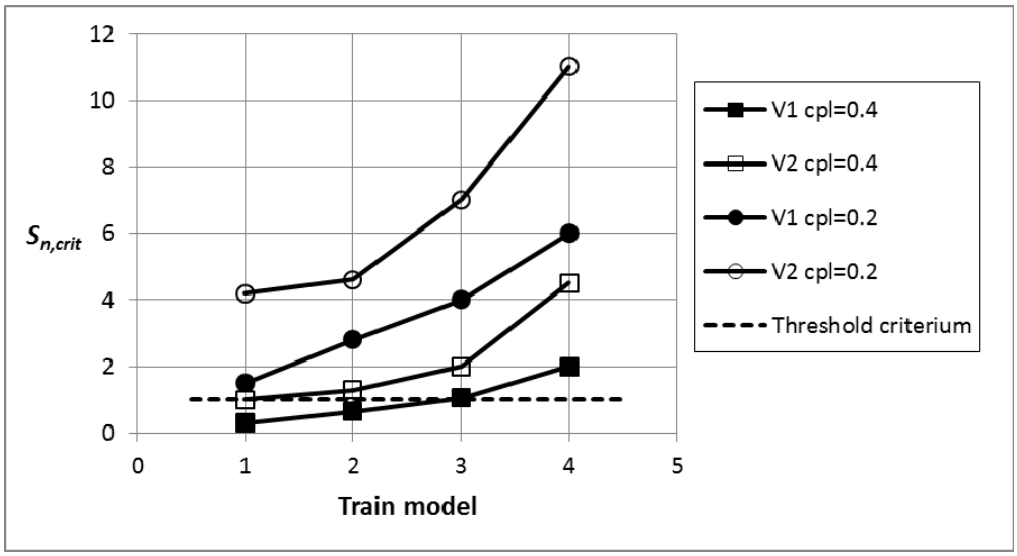

Figure 4. Critical angular impulse, which occurs once, as function of the train models 1, 2, 3, and 4, for both tracks V1 and V2, and for two values of c_{pl} (0.2 and 0.4). Threshold criterium for initiation of the stone rolling.

It can be shown that, if a threshold for a critical value of the angular impulse is defined (based on the ballast size, the size, the stone density and the orientation on the track), some trains would not excite ballast pick-up (trains 1 and 2); another would exhibit a marginal behaviour (train 3), whilst train 4 would definitely excite ballast motion.

4 CONCLUSIONS

The main parameters influencing the phenomenon of the starting of the stone rotation motion have been identified, by developing a theoretical model of the effect of wind on bodies lying on a flat floor. On the other hand, the relationship among these parameters that leads to a successful motion has been obtained. Two limits exist, for long and short duration gusts, respectively.

In order to meet the need of creating suitable wind gusts (with sinusoidal time variation) to check the theoretical model predictions, a wind tunnel with a gust generation mechanism has been set-up. A great flexibility has been considered in the wind tunnel design to allow the change of the parameters involved such as: flow quality conditioning elements at the entrance of the test chamber, which allows to obtain flows with several turbulence intensities and profile uniformity, several gust amplitudes, continuous values of mean wind speed and gust frequency, and an easily accessible gate to change stone models or to include other mechanisms. A good agreement between the time variation of speed signals measured in the wind tunnel chamber and the theoretical sinusoidal approximation has been obtained at the gust wind tunnel. The experimental results concerning stone motion initiation angle have to be placed in the region between the low frequency gust case (lower limit) and the steady speed case (upper limit) which coincides with high frequency gust case. As velocity increases, experimental results show a better agreement with theoretical predictions, which could be explained remembering that the higher the velocity the lower the starting angle, and consequently the linearization approximation considered in the derivation of the theoretical results is more realistic.

Other test campaign has been developed, but this one on the track. The effect on the ballast of the flow generated by the train is studied in these tests by measuring the pressure load due to this flow acting on a model stone equipped with pressure taps and placed on the

ballast bed. In parallel with the pressure measurements, the wheel passes were also detected by using a light barrier, in order to synchronize the pressure measurements with the actual train geometry. A simplified theoretical method to calculate the angular impulse produced on the ballast stone has been used, and some statistical results have been obtained with several passes of the same train model circulating by a track. The vertical acceleration on the sleeper center has also been recorded, aiming at to obtain experimental data that can help to the study of the action of the sleeper vibration on the initiation of the rotation of the ballast lying on it.

A new method has been developed to study the effect on the ballast of the flow generated by the train. The feasibility of this method has being showed based on the measurement analysis of the Madrid – Barcelona High Speed Line campaign, whose aim is to obtain a number of data large enough to support statistical significance. From the analysis of the results, contributions to the development of a new identification method of train-ballast interaction characteristics are expected, which is crucial for standardization of train interoperability.

5 ACKNOWLEDGEMENTS

The study covered in this paper has been carried out under financial support from Administracion de Infraestructuras Ferroviarias (ADIF) and Patentes Talgo S.A. The authors would like to thank Emilio García and David Pérez Rodriguez from Patentes Talgo S.A. for fruitful discussions and suggestions.

6 REFERENCES

Bagnold, R.A., 1941. The physics of blown sand and desert dunes. Chapman and Hall, London.

Kwon, H.B., Park, C.S., 2006. An experimental study on the relationship between ballast-flying phenomenon and strong wind under high-speed train. Proceedings of the 7th World Congress on Railway Research, Montreal, Canada.

Nalpanis, P., Hunt, J.C., Barret, C.F., 1993. Saltating particles over flat beds. Journal of Fluid Mechanics 251, 661-685.

Owen, P.R., 1964. Saltation of uniform grains in air. Journal of Fluid Mechanics 20 (2), 225-242.

Quinn, A.D., Hayward, M., Baker, C.J., Schmid, F., Priest, J.A., Powrie, W., 2009. A full-scale experimental and modelling study of ballast flight under high speed trains. Journal of Rail Rapid Transit, Proceedings of the Institution of Mechanical Engineers 224 (F2), 61-74.

Sanz-Andres, A., Navarro-Medina, F., 2010. The initiation of rotational motion of a lying object caused by wind gusts. Journal of Wind Engineering and Industrial Aerodynamics 98, 772-783.

Zhang, W., Kang, J.H., Lee, S.J., 2007. Tracking of saltating sand trajectories over a flat surface embedded in an atmospheric boundary layer. Geomorphology 86, 320-331.